Two-dimensional simulation by regularization of free surface viscoplastic flows with Drucker-Prager yield stress, application to granular collapse

Christelle Lusso
CERMICS/IPGP/LMD
lussoc@lmd.ens.fr

31 mars 2015

Plan

1. Introduction
2. Drucker–Prager model
3. 1D/2D comparison
4. Simulation of granular collapse
5. Conclusions

- Geophysical flows modeling : avalanches, landslides, pyroclastic flows.
- Study of the fluid/solid transition in a two-phase fluid.
- Dynamics with motionless part at the bottom and mobile on the surface.

Main difficulties :

- Rheology : - plasticity and viscosity,
  - yield stress, transition.
- Free surface.

Yield stress fluid

Features :

- Existence of a flow threshold.
- Below the yield limit, the stress cannot cause the flow.

Phase transition

Simultaneous existence :

static part & mobile part.

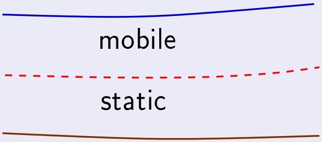

Viscoplastic rheology

- $\vec{U}$ velocity, p pressure.
- Stress tensor : $P = \sigma - p\mathrm{Id}$, $\mathrm{tr}\sigma = 0$.

Viscoplastic law ⇒ yield criterion

- Bingham law :

$$\begin{aligned} \sigma = 2\eta D\vec{U} + \boldsymbol{\sigma_c} \frac{D\vec{U}}{||D\vec{U}||} \quad & \text{if } D\vec{U} \neq 0, \\ \|\sigma\| \leq \boldsymbol{\sigma_c},\ \sigma \text{ symmetric} \quad & \text{if } D\vec{U} = 0, \end{aligned}$$

  with $D\vec{U}$ the strain tensor and η the viscosity.

- **Drucker–Prager** law :

$$\begin{aligned} \sigma = 2\eta D\vec{U} + \boldsymbol{\kappa(p)} \frac{D\vec{U}}{||D\vec{U}||} \quad & \text{if } D\vec{U} \neq 0, \\ ||\sigma|| \leq \boldsymbol{\kappa(p)},\ \sigma \text{ symmetric} \quad & \text{if } D\vec{U} = 0, \end{aligned}$$

  with $\kappa(p)$ the plasticity.

Plan

1 Introduction

2 Drucker–Prager model
- Model formulation
- Regularization and variational formulation
- Discretization

3 1D/2D comparison

4 Simulation of granular collapse

5 Conclusions

Domain description

- The domain Ω_t is time dependent (**free surface $\Gamma_{f,t}$**).
- Fluid/solid **interface** between the two phases, characterized by $D\vec{U}$ zero or $D\vec{U}$ nonzero.
- The **interface** is not described explicitly.
- Fixed **bottom Γ_b**.

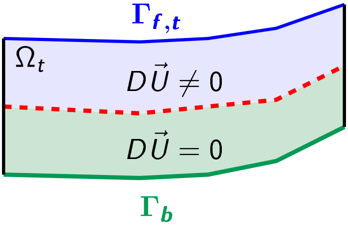

- Boundary condition : $P.\vec{N} = \gamma\vec{N}$ on $\Gamma_{f,t}$ and $\vec{U} = 0$ on Γ_b.
- Kinematic condition : $N_t + \vec{N} \cdot \vec{U} = 0$ on $\Gamma_{f,t}$.

Conservation equations

- **Incompressible** Navier–Stokes equations :

$$\begin{aligned} \rho\left(\partial_t \vec{U} + (\vec{U}.\nabla_{\vec{X}})\vec{U}\right) + \mathrm{div}_{\vec{X}} P &= \rho \vec{f} \quad \text{in }]0,T[\times\Omega_t, \\ \mathrm{div}_{\vec{X}} \vec{U} &= 0 \quad \text{in }]0,T[\times\Omega_t. \end{aligned}$$

- **Viscoplastic** fluid of Bingham type :

$$\begin{aligned} \sigma &= 2\eta D\vec{U} + \kappa(p)\frac{D\vec{U}}{\|D\vec{U}\|} && \text{if } D\vec{U} \neq 0, \\ \|\sigma\| &\leq \kappa(p),\ \sigma \text{ symmetric} && \text{if } D\vec{U} = 0, \end{aligned}$$

where $D\vec{U} = \frac{\nabla\vec{U}+\nabla\vec{U}^t}{2}$.

- Drucker–Prager relation :

$$\kappa(p) = \sqrt{2}\mu_s[p]_+,$$

μ_s internal friction coefficient.

Geometry and boundary conditions (a)-(b)

Periodic flow over an inclined rigid bed (a)

- No-slip condition at the **bottom** : $\vec{U}(t, \vec{X}) = 0$ on $\boldsymbol{\Gamma_b}$.
- Periodicity condition on the **lateral side** $\boldsymbol{\Gamma_{l,t}} \cup \boldsymbol{\Gamma_{r,t}}$.

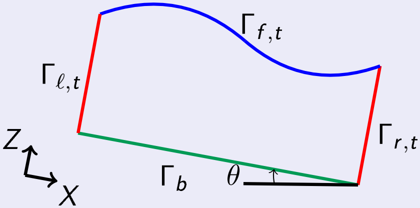

- No-stress condition at the **free surface** : $P \cdot \vec{N} = 0$ on $\boldsymbol{\Gamma_{f,t}}$.
- Kinematic condition at the **free surface** : $N_t + \vec{N} \cdot \vec{U} = 0$ on $\boldsymbol{\Gamma_{f,t}}$.
- Initial condition : $\vec{U}(0, \vec{X}) = \vec{U}_0(\vec{X})$.

Collapse over a rigid (b)/erodible (b_e) bed

- No-penetration condition :
$\vec{U}(t,\vec{X})\cdot\vec{N}=0$ on $\Gamma_{b,t}\cup\Gamma_{\ell,t}$.
- Coulomb friction condition :

$$\sigma_T = -\mu_{b/\ell}\frac{\vec{U}_T}{|\vec{U}_T|}[p-P_N]_+ \quad \text{if } \vec{U}_T\neq 0.$$
$$|\sigma_T| \leq \mu_{b/\ell}[p-P_N]_+ \quad \text{if } \vec{U}_T = 0.$$

on $\Gamma_{b,t}\cup\Gamma_{\ell,t}$.

Friction coefficient : $\mu_{b/\ell}=\mu_b$ on $\Gamma_{b,t}$,
$\mu_{b/\ell}=\mu_\ell$ on $\Gamma_{\ell,t}$.

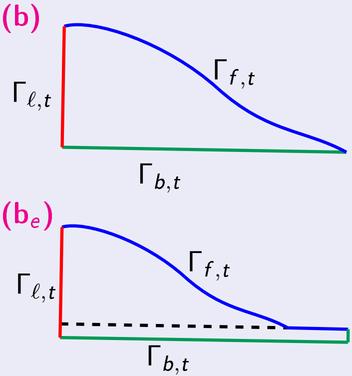

- (b) : No-stress condition : $P\cdot\vec{N}=0$ on $\Gamma_{f,t}$.
- (b_e) : Local surface tension : $P\cdot\vec{N}=\gamma\vec{N}$ on $\Gamma_{f,t}$.
- Kinematic condition on $\Gamma_{f,t}$ and initial condition.

Plan

1. Introduction

2. Drucker–Prager model
   - Model formulation
   - Regularization and variational formulation
   - Discretization

3. 1D/2D comparison

4. Simulation of granular collapse

5. Conclusions

Regularization

Motivation :

Regularization $\Downarrow$ variational equation **VS** Augmented Lagrangian $\Downarrow$ variational inequation

Regularized constitutive equation :

$$\sigma_{\epsilon} = 2\eta D\vec{U} + \kappa(p)\frac{D\vec{U}}{\sqrt{||D\vec{U}||^2 + \epsilon^2}}, \qquad \mathbf{0} < \epsilon \ll \mathbf{1},$$

with $\kappa(p) = \sqrt{2}\mu_s[p]_+$.

Spaces

We consider

$$\boldsymbol{V} := \left\{ \vec{V} \in L^2(0,T;\boldsymbol{V}_{\boldsymbol{t}}) \;\middle|\; \frac{d\vec{V}}{dt} \in L^2(0,T;\boldsymbol{V}'_t) \right\},$$
$$M := L^2(0,T;\boldsymbol{M}_{\boldsymbol{t}}),$$

with

(a) $\boldsymbol{V}_{\boldsymbol{t}} := \left\{ \vec{V} \in H^1(\Omega_{\boldsymbol{t}})^2 \;\middle|\; \vec{V} = \boldsymbol{0} \text{ on } \Gamma_{\boldsymbol{b}},\ \vec{V}(\vec{X}) = \vec{V}(\mathcal{T}(\vec{X})) \text{ for } \vec{X} \in \Gamma_{\ell,\boldsymbol{t}} \right\},$

(b) $\boldsymbol{V}_{\boldsymbol{t}} := \left\{ \vec{V} \in H^1(\Omega_{\boldsymbol{t}})^2 \;\middle|\; \vec{V} \cdot \boldsymbol{N} = 0 \text{ on } \Gamma_{\boldsymbol{b},\boldsymbol{t}} \cup \Gamma_{\ell,\boldsymbol{t}} \right\},$

and $\boldsymbol{M}_{\boldsymbol{t}} = L^2(\Omega_t)$.

Variational formulation

Find $(\vec{U}, p) \in \boldsymbol{V} \times M$ such that for almost all $t \in (0, T)$, and all $(\vec{V}, q) \in \boldsymbol{V}_t \times M_t$,

$$\int_{\Omega_t} \rho \left(\partial_t \vec{U} + (\vec{U} \cdot \nabla)\vec{U}\right) \cdot \vec{V} + \int_{\Omega_t} 2\eta D\vec{U} : D\vec{V} + \int_{\Omega_t} \kappa(p) \frac{D\vec{U}}{\sqrt{||D\vec{U}||^2 + \epsilon^2}} : D\vec{V}$$

$$- \int_{\Omega_t} p \,\mathrm{div}\, \vec{V} + \int_{\Gamma_{b,t} \cup \Gamma_{\ell,t}} \mu_{b/\ell} \frac{\vec{U}_T \cdot \vec{V}}{\sqrt{|\vec{U}_T|^2 + \epsilon_f^2}} [p - P_N]_+ = \int_{\Omega_t} \rho \boldsymbol{f} \cdot \vec{V} + \int_{\Gamma_{f,t}} \gamma \vec{V} \cdot \vec{N},$$

$$\int_{\Omega_t} q \,\mathrm{div}\, \vec{U} = 0.$$

(a) : - $\mu_{b/\ell} = 0$ (no friction),
- $\gamma = 0$ (no surface tension).

(b) : $\mu_{b/\ell} > 0$ (Coulomb friction).

(b_e) : $\gamma > 0$ (local surface tension).

Displacement of the domain

$\hat{\Omega}$: reference domain

Ω_t : current domain

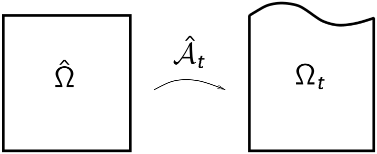

Domain velocity :

$$\vec{W}(t,x) = \frac{\partial \hat{\mathcal{A}}_t}{\partial t}(\hat{x}), \text{ with } \hat{x} = \hat{\mathcal{A}}_t^{-1}(x).$$

Time derivative treatement :

$$\int_{\Omega_t} \partial_t \vec{U} \cdot \vec{V} = \int_{\Omega_t} \partial_t((\vec{U} \cdot \vec{V}) \circ \hat{\mathcal{A}}_t) \circ \hat{\mathcal{A}}_t^{-1} - \int_{\Omega_t} ((\vec{W} \cdot \nabla)\vec{U}) \cdot \vec{V}.$$

for $\vec{V}$ such as $\vec{V}(t,x) = \vec{\hat{V}}(\hat{\mathcal{A}}_t^{-1}(x))$.

J. F. Gerbeau, C. Le Bris, T. Lelievre, *Mathematical methods for the magnetohydrodynamics of liquid metals*, Oxford University Press, 2006.

Determination of $\vec{W}$

- We solve an elliptic problem inside Ω_t :

$$-\operatorname{div}(D\vec{W}) = 0 \quad \text{in } \Omega_t.$$

- We extend suitable boundary values consistent with the kinematic BC :
  - Boundary conditions **(a)** :

$$\begin{aligned}(\vec{W} - \vec{U}) \cdot \vec{N} &= 0 \quad \text{on } \boldsymbol{\Gamma_b} \cup \boldsymbol{\Gamma_{f,t}},\\ \vec{W} \cdot \vec{N} &= 0 \quad \text{on } \boldsymbol{\Gamma_{\ell,t}} \cup \boldsymbol{\Gamma_{r,t}},\\ (D\vec{W}\vec{N})_T &= 0 \quad \text{on } \boldsymbol{\Gamma}.\end{aligned}$$

  - Boundary conditions **(b)** :

$$\begin{aligned}(\vec{W} - \vec{U}) \cdot \vec{N} &= 0 \quad \text{on } \boldsymbol{\Gamma},\\ (D\vec{W}\vec{N})_T &= 0 \quad \text{on } \boldsymbol{\Gamma}.\end{aligned}$$

Plan

1 Introduction

2 Drucker–Prager model
- Model formulation
- Regularization and variational formulation
- Discretization

3 1D/2D comparison

4 Simulation of granular collapse

5 Conclusions

Discretization

- **Mesh mapping :**

$$\mathcal{A}_{n,n+1} : \Omega^n \to \Omega^{n+1}$$
$$\vec{X} \mapsto \vec{X} + \Delta t_n \vec{W}^n(\vec{X}).$$

- **Time derivative discretization :**

$$\int_{\Omega_t} \partial_t \vec{U} \cdot \vec{V} = \int_{\Omega^{n+1}} \left(\frac{\vec{U}^{n+1} - \vec{U}^n \circ \mathcal{A}^{-1}_{n,n+1}}{\Delta t} - \vec{W}^n \circ \mathcal{A}^{-1}_{n,n+1} \cdot \nabla \vec{U}^{n+1} \right) \cdot \vec{V} + O(\Delta t).$$

- $V^n = H^1_{\mathrm{bc}}(\Omega_{t^n})$ and $M^n = L^2(\Omega_{t^n})$.

- Given $(\vec{U}^{n+1,k}, p^{n+1,k})$, find $(\vec{U}^{n+1,k+1}, p^{n+1,k+1}) \in \boldsymbol{V}^{n+1} \times M^{n+1}$ such that for all $(\vec{V}, q) \in \boldsymbol{V}^{n+1} \times M^{n+1}$,

$$\int_{\Omega^{n+1}} \rho \left(\frac{\vec{U}^{n+1,k+1} - \vec{U}^n \circ \mathcal{A}^{-1}_{n,n+1}}{\Delta t_n} + \left[\left(\vec{U}^{n+1,k} - \vec{W}^n \circ \mathcal{A}^{-1}_{n,n+1} \right) \cdot \nabla \right] \vec{U}^{n+1,k+1} \right) \cdot \vec{V}$$

$$+ \int_{\Omega^{n+1}} \left(2\eta + \frac{\kappa^{n+1,k}}{\sqrt{\|D\vec{U}^{n+1,k}\|^2 + \epsilon^2}} \right) D\vec{U}^{n+1,k+1} : D\vec{V}$$

$$- \int_{\Omega^{n+1}} p^{n+1,k+1} \operatorname{div} \vec{V} + \int_{\Gamma_b^{n+1} \cup \Gamma_\ell^{n+1}} \mu_{b/\ell} \frac{\vec{U}_T^{n+1,k+1} \cdot \vec{V}}{\sqrt{|\vec{U}_T^{n+1,k}|^2 + \epsilon_f^2}} [p^{n+1,k} - P_N^{n+1,k}]_+$$

$$+ \int_{\Gamma_b^{n+1} \cup \Gamma_\ell^{n+1}} \xi (\vec{U}^{n+1,k+1} \cdot \boldsymbol{N})(\vec{V} \cdot \boldsymbol{N}) = \int_{\Omega^{n+1}} \rho \boldsymbol{f}^{n+1} \cdot \vec{V} + \int_{\Gamma_f^{n+1}} \gamma \vec{V} \cdot \boldsymbol{N},$$

$$\int_{\Omega^{n+1}} q \operatorname{div} \vec{U}^{n+1,k+1} = 0,$$

  - $\kappa^{n+1,k} = \sqrt{2}\mu_s [p^{n+1,k}]_+$,
  - $\xi \gg 1$ penalty parameter ($\xi = 0$ in case (a)).

- **Space discretization :** $\mathbb{P}_2/\mathbb{P}_1$ finite element (Taylor-Hood).

Domain velocity $\vec{W}_h^n$

We look for $\vec{W}_h^n \in \mathbb{P}_2(\Omega_h^n)^2$ such that for all $\vec{V}_h \in \mathbb{P}_2(\Omega_h^n)^2$,

$$\int_{\Omega_h^n} D\vec{W}_h^n : D\vec{V}_h + \int_{\Gamma_h^n} \hat{\xi}(\vec{W}_h^n - \vec{U}_h^n)\cdot \boldsymbol{N}\,(\vec{V}_h \cdot \boldsymbol{N}) = 0,$$

$\hat{\xi} \gg 1$ penalty parameter.

(a) $\boldsymbol{\Gamma} = \boldsymbol{\Gamma_b} \cup \boldsymbol{\Gamma_{f,t}}$,
(b) $\boldsymbol{\Gamma} = \boldsymbol{\Gamma}$.

Update Algorithm

- We suppose that Ω_h^n, $\vec{U}_h^n$, p_h^n are known and we compute $\vec{W}_h^n$.
- We move the nodes of the mesh according to $\mathcal{A}_{n,n+1}$.
  In case **(b)** we may need to limit the time step so that the free surface nodes do not cross the bottom :

  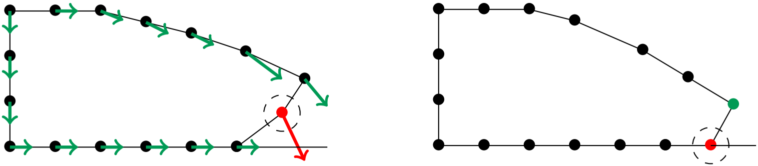

  Thus we obtain Ω_h^{n+1}.
- Finally, we compute $(\vec{U}_h^{n+1}, p_h^{n+1})$ on Ω_h^{n+1}.

Surface tension (b_e)

Difficulty : erodible bed geometry $\Rightarrow$ folding up of the free surface.

Key : apply local surface tension with $\gamma = \gamma_0 \mathcal{C}$:
- $\gamma_0 = o(h)$ with h the mesh size,
- $\mathcal{C} = d\theta/ds$ **local curvature** of the free surface.

Numerical approximation :

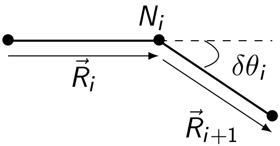

N_i free surface nodes.
$\vec{R}_i = \overrightarrow{N_{i-1}N_i}$.
$\delta\theta_i$ angular variation.

$$\mathcal{C}_i = \frac{\delta\theta_i}{\left(|\vec{R}_{i+1}| + |\vec{R}_i|\right)/2}$$

curvature at N_i.

- 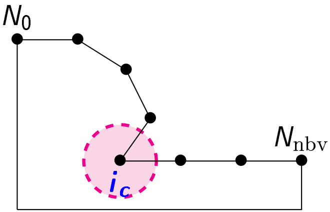

$\mathcal{C}_i$ is largest in i_c

- we apply surface tension around i_c of extension $\delta > 0$

$$\gamma_{0,i} = \overline{\gamma}_0 \left(\max\left\{ 0, 1 - \left(\frac{i - i_c}{\delta} \right)^2 \right\} \right)^2 .$$

Validity test

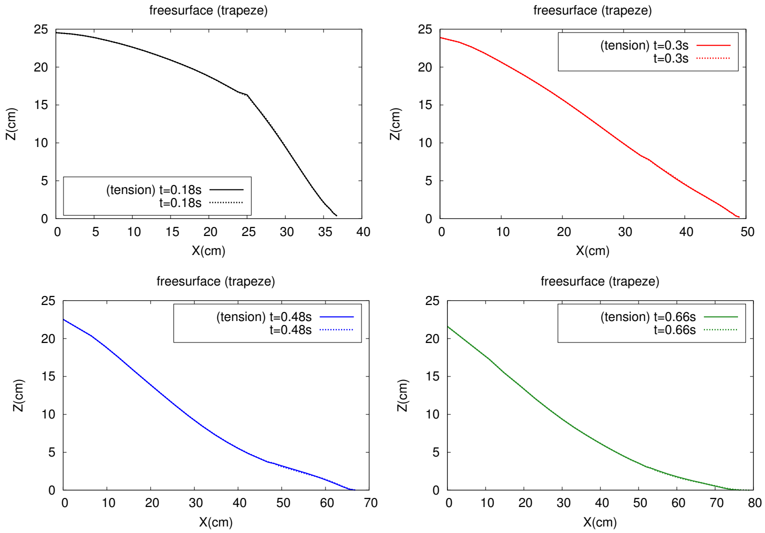

Figure: Comparison between regularization method with surface tension (full lines) and regularization method without surface tension (dotted lines).

Plan

1. Introduction
2. Drucker–Prager model
3. 1D/2D comparison
4. Simulation of granular collapse
5. Conclusions

Model with source term (S)

Assumptions :

- Change of coordinates $\vec{X} \mapsto (X, Z)$,
- shallow water assumptions,
- X parameter.

Simplified model [1]

$$
\begin{aligned}
\partial_t U(t,Z) + \mathbf{S(t,Z)} - \nu \partial^2_{ZZ} U(t,Z) &= 0 \quad \forall Z \in]b(t), h[,\\
U &= 0 \quad \text{at } Z = b(t),\\
\nu \partial_Z U &= 0 \quad \text{at } Z = b(t),\\
\nu \partial_Z U &= 0 \quad \text{at } Z = h.
\end{aligned}
$$

[1] *Modélisation numérique des écoulements gravitaires viscoplastiques avec transition fluide/solide*, PhD thesis. Université Paris-Est, Champs-sur-Marne, 2013.

Case (a) : uniform flow with plug

- Longitudinal velocity $U(t, Z)$ solving **(S)**,
- $\boldsymbol{S(t, Z)} = g \cos\theta(\mu_s - \tan\theta)$ constant source term,
- θ angle of inclined domain Ω.

$\mu_s > \tan\theta \Longrightarrow$
- $\vec{U} = (U, 0)$ solution of **(NSDP)** with BC (a),
- the pressure is hydrostatic : $p = g \cos\theta(h - Z)$.

Velocity error :

- $U(t, Z)$ extended on the 2D mesh,
- error between U and the longitudinal component of $\vec{U}$.

Numerical results

- $\epsilon = 10^{-2}$: regularization error dominates.
- $\epsilon = 10^{-6}$: regularization error dominated by discretization error.
- Numerical convergence of order 1 in space and in time.

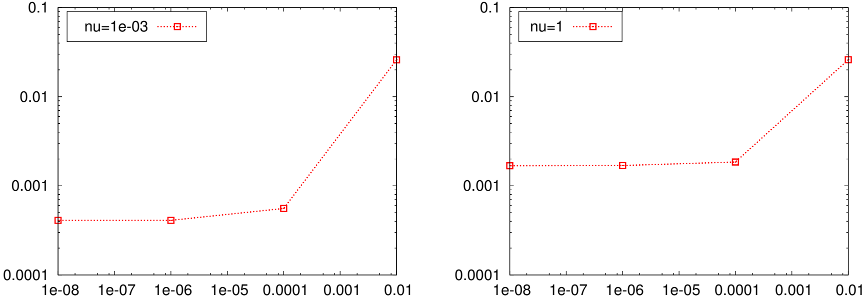

Figure: Velocity error with respect to ϵ.

ϵ	10^{-2}	10^{-4}	10^{-6}	10^{-8}
total iter	824	2958	5086	5272

$\epsilon = 10^{-8} \Longrightarrow$ saturation of iterations cost.

Plan

1. Introduction
2. Drucker–Prager model
3. 1D/2D comparison
4. Simulation of granular collapse
5. Conclusions

Case (b) : collapse over horizontal plane

Comparison of numerical results with :

- Numerical results from **augmented Lagrangian** formulation [1].
- Experimental results from **laboratory experiments** [2].

Profiles

- Thickness profile (**free surface** evolution).
- Components of velocity profiles U_X and U_Z.
- Position of the static/flowing **interface**.

[1] D. Bresch, E. D. Fernandez-Nieto, I. Ionescu, P. Vigneaux, *Augmented Lagrangian Method and Compressible Visco-Plastic Flows : Applications to Shallow Dense Avalanches*, Advances in Mathematical Fluid Mechanics, 2010.

[2] M. Farin, A. Mangeney, O. Roche, *Fundamental changes of granular flow dynamics, deposition, and erosion processes at high slope angles : Insights from laboratory experiments*, J. Geophys. Res. Earth Surf., 2014.

Configuration

Physic parameters :

- $\mu_s = \tan 25.5^\circ$,
- $\mu_b = \tan 25.5^\circ$,
- $\mu_l = \tan 10.2^\circ$,
- $\eta = 1\mathrm{Pa.s}$,
- $\rho = 1550\mathrm{kg.m}^{-3}$.

Geometric parameters :

- $\alpha_0 = 70^\circ$,
- $h_0 = 25\mathrm{cm}$,
- $h_e = 5\mathrm{mm}$,
- $l_0 = 29.7\mathrm{cm}(\mathrm{I})/80\mathrm{cm}(\mathrm{II})$.

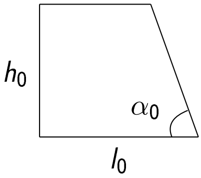

(I) rigid bed

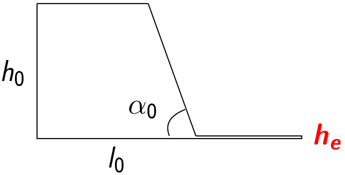

(II) erodible bed

Meshes

Initial mesh :

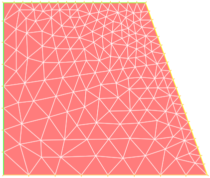

Final mesh :

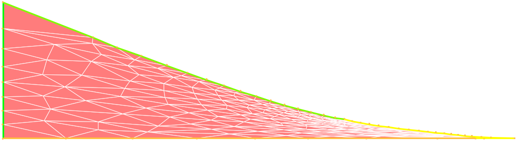

Figure: Initial and final ($t \geq 0.7$s) meshes for the regularization method with $\epsilon = 10^{-6}\text{s}^{-1}$.

Plan

1. Introduction
2. Drucker–Prager model
3. 1D/2D comparison
4. Simulation of granular collapse
   - Comparison with augmented Lagrangian method
   - Comparison with laboratory experiments
   - Sensitivity with respect to ϵ
5. Conclusions

Freesurface

Parameters : - $\epsilon = \epsilon_f = 10^{-6}\mathrm{s}^{-1}$.
- $\Delta X \simeq 10^{-2}\mathrm{m}$, $\Delta t = 10^{-3}\mathrm{s}$, and $\varepsilon_{\mathrm{stop}} = 10^{-3}$.

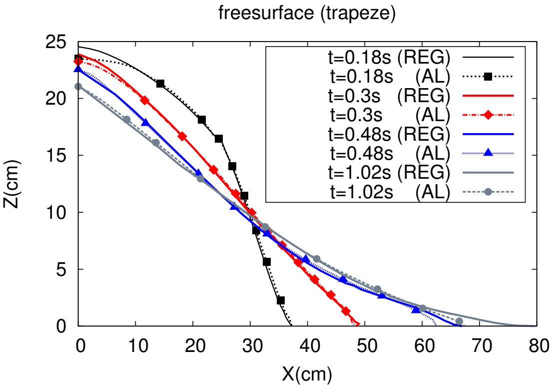

The regularization method leads to :
- less decreasing thickness on the left side,
- slightly faster front propagation (on the right),
- **7 times faster running**.

Velocity components U_X and U_Z

Vertical sections : $X_g - 10$cm and X_g ($X_g = 29.7$cm front position).

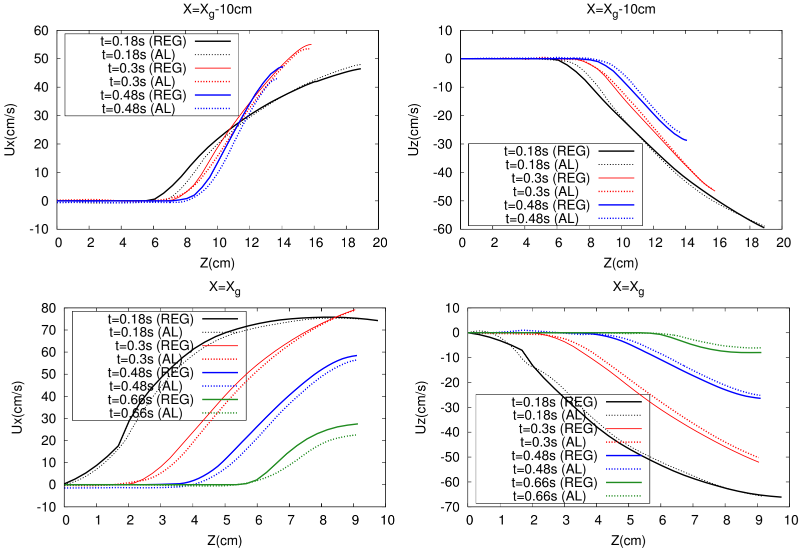

Static/flowing interface

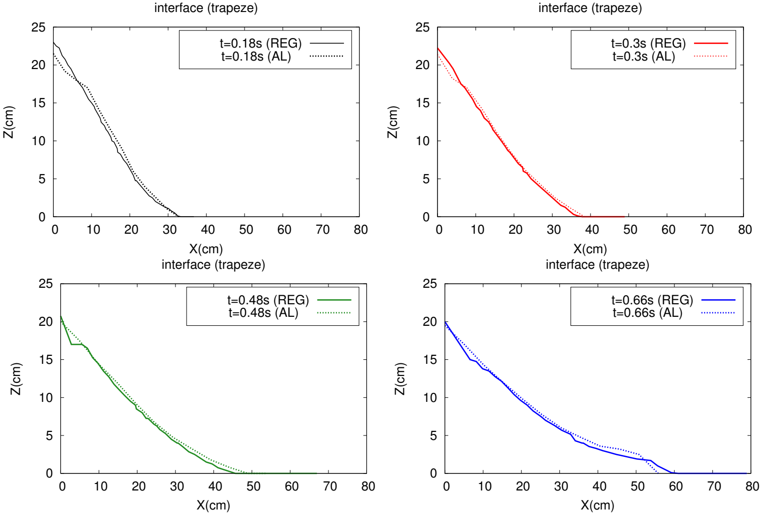

Interface approximation : - vertical sections $X_i \in [0, X_t^{\max}]$, with $X_t^{\max}$ the Ω_t length,
- $\underline{\lim}\left\{y \in [0, h(t, X_i)] \;\middle|\; |\vec{U}(X_i, y)| > \varepsilon_{\vec{U}}\right\}$, $\varepsilon_{\vec{U}} = 10^{-3}\text{m.s}^{-1}$.

Plan

1. Introduction
2. Drucker–Prager model
3. 1D/2D comparison
4. Simulation of granular collapse
   - Comparison with augmented Lagrangian method
   - Comparison with laboratory experiments
   - Sensitivity with respect to ϵ
5. Conclusions

Freesurface

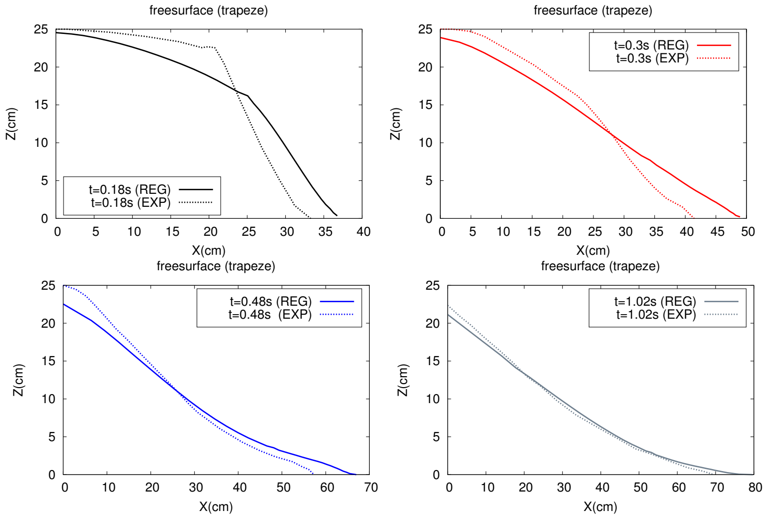

The regularization method leads to :
- faster dynamics than in experiments,
- final deposit very well approximated.

Velocity components U_X and U_Z

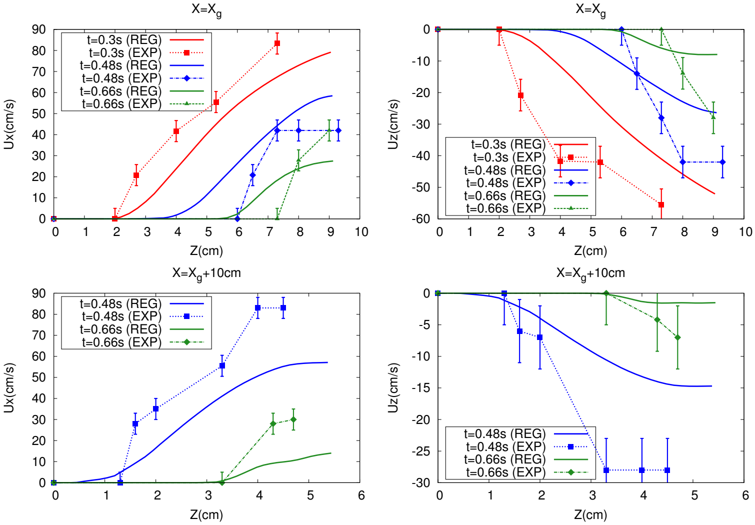

The regularization method leads to :

- velocity profiles qualitatively reproduced,
- maximum horizontal velocity close to free surface.

Static/flowing interface

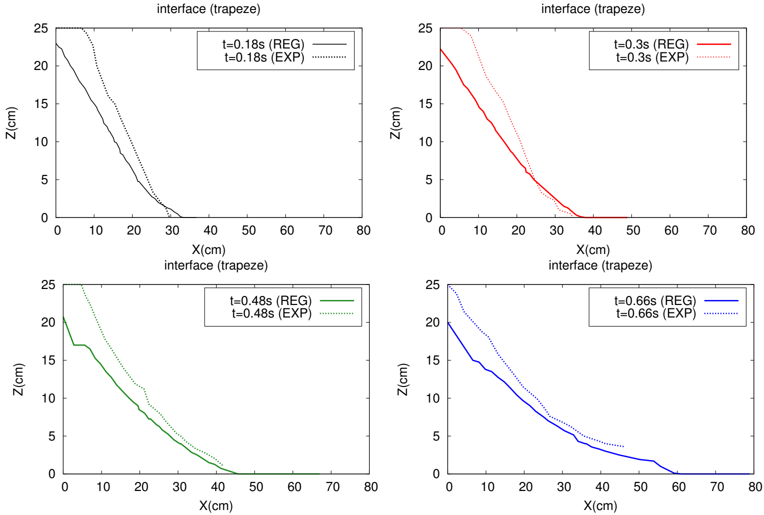

The regularization method leads to :
- overall good approximation of interface position,
- position underestimated on top of the left side.

Erodible bed

Framework : erosion process modeling.

Goal : simulation of a granular collapse over an erodible bed made of the same material represented by a thin layer of thickness $\boldsymbol{h_e = 5\text{mm}}$ under the trapezoidal column.

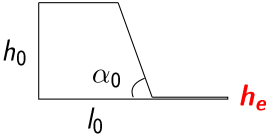

Mean : local surface tension effects.

Freesurface

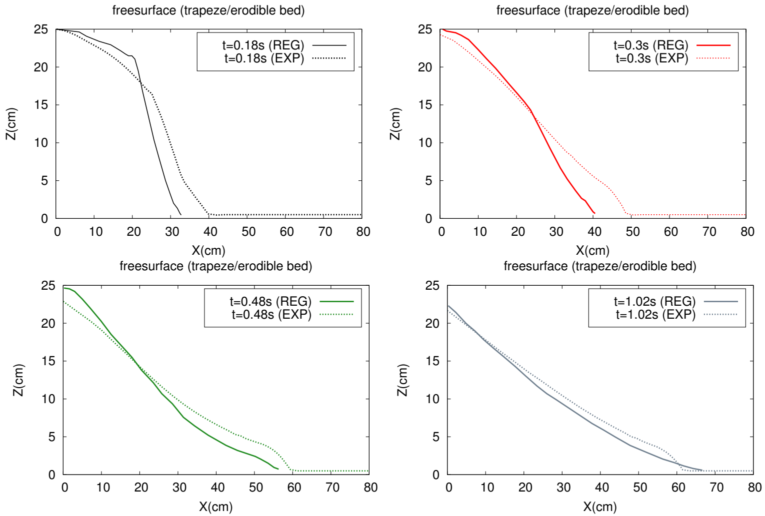

The regularization method with **local surface tension** leads to :

- comparable profiles all along the simulation,
- final deposit well approximated.

Plan

1 Introduction

2 Drucker–Prager model

3 1D/2D comparison

4 Simulation of granular collapse
- Comparison with augmented Lagrangian method
- Comparison with laboratory experiments
- Sensitivity with respect to ϵ

5 Conclusions

Sensitivity with respect to ϵ

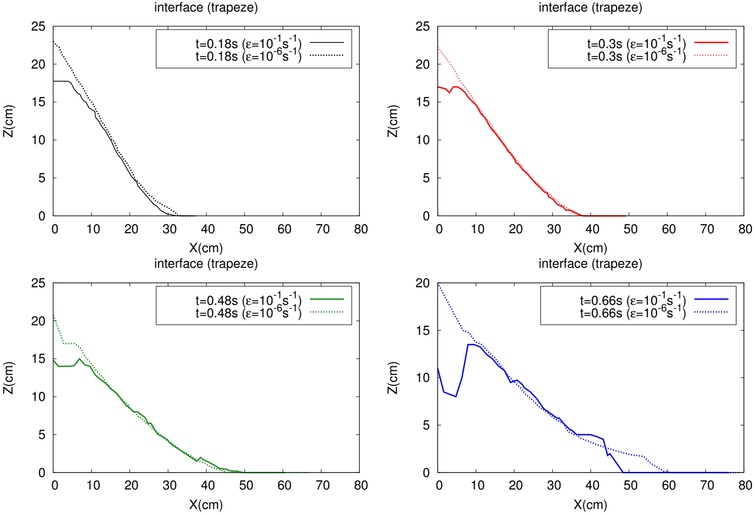

Figure: Comparison of the static/flowing interface between the regularization method with $\epsilon = 10^{-1}\mathrm{s}^{-1}$ and with $\epsilon = 10^{-6}\mathrm{s}^{-1}$.

Plan

1. Introduction
2. Drucker–Prager model
3. 1D/2D comparison
4. Simulation of granular collapse
5. Conclusions

Conclusions

- Two-dimensional flows of **viscoplastic** materials with **pressure-dependent** yield stress.
- **Regularization** method with **evolution** of the mesh.
- **Validation** : simple shear flow configuration and comparison with augmented Lagrangian method.
- Regularization **runs faster** than augmented Lagrangian.
- Geophysically relevant configurations : **granular collapse**.
- **Erosion** process simulation.

Perspectives

- Adaptive mesh.
- Inclined plane.
- Rectangle geometry.
- Viscosity pressure-rate dependent.
- Friction pressure-rate dependent.

Merci ! !